

Effect of Plasma on Shadow of Non-singular Rotating Magnetic Monopole in Perfect Fluid Dark matter

Gowtham Sidharth M, Dr. Sanjit Das

March 20, 2022

Overview

- Introduction
- Bardeen Blackhole in PFDM
- Shadow of Bardeen Blackhole in PFDM
- Photon orbits for Blackhole Immersed in Plasma
- Shadows
- Inference

Introduction

- In an ordinary world,
- Shadows are common phenomena
- shadows are kind of omnipresent
- shadows are there when there is light
- boundaries separate dark and illuminated regions

Introduction

- In General Relativity,
- Black holes tend to suck up surrounding matter in a process called 'accretion'.
- This surrounding matter accreting onto the black hole heats up through viscous dissipation and converts gravitational energy into radiation, radiating bright light at many frequencies, including radio waves that can be picked up by radio telescopes.
- This shining material accreting onto the black hole crosses the event horizon, resulting in a dark area over a bright background: this is the so-called black hole "shadow".
- The shadow is essentially an image of the event horizon, lensed by the strong gravitational field around the BH and superimposed over the background light.

Introduction



Bardeen Blackhole in PFDM

- In 1960 Roger Penrose proposed his cosmic censorship conjecture.
- The conjecture does not prevent the existence of blackhole which are free of singularity
- Bardeen blackhole are such non singular blackholes.

$$ds^2 = -\left(1 - \frac{2Mr^2}{(r^2 + g^2)^{3/2}}\right)dt^2 + \left(1 - \frac{2Mr^2}{(r^2 + g^2)^{3/2}}\right)dr^2 + r^2d\Omega^2 \quad (1)$$

- where g is the monopole of self gravitating magnetic field described by non-linear electrodynamics
- Bardeen model describes regular space time,with curvature Invariants which are all regular everywhere.
- For certain range of parameter g , the Bardeen metric also describes a blackhole.

Bardeen Blackhole in PFDM

- In presence of perfect fluid dark matter, Given the coupling between gravitational field and non-linear electromagnetic field, the Einstein Maxwell equation is modified as,

$$G_{\mu}^{\nu} = 2\left(\frac{\partial \mathcal{L}}{\partial F} F_{\mu\lambda} F^{\mu\lambda} - \delta_{\mu}^{\nu}\right) + 8\pi T_{\mu}^{\nu}(\text{PFDM}) \quad (2)$$

and \mathcal{L} is given by

$$\mathcal{L} = \frac{3M}{|g|^3} \left(\frac{\sqrt{2g^2 F}}{1 + \sqrt{2g^2 F}} \right)^{3/2} \quad (3)$$

- The solution for this will give us the metric for Bardeen blackhole in PFDM

$$ds^2 = -\left(1 - \frac{2Mr^2}{(r^2 + g^2)^{3/2}} + \frac{\omega}{r} \ln \frac{r}{|\omega|}\right) dt^2 + \left(1 - \frac{2Mr^2}{(r^2 + g^2)^{3/2}} + \frac{\omega}{r} \ln \frac{r}{|\omega|}\right)^{-1} dr^2 + r^2 d\Omega^2 \quad (4)$$

Photon orbits

The rotating Bardeen metric in perfect fluid dark matter is obtained with the help of Newman-Janis Algorithm;

$$ds^2 = -\left(1 - \frac{2\rho r}{\Sigma}\right)dt^2 + \frac{\Sigma}{\Delta}dr^2 + \Sigma d\theta^2 - \frac{4a\rho r \sin^2\theta}{\Sigma} dt d\phi + \sin^2\theta \left(r^2 + a^2 + \frac{2a^2\rho r \sin^2\theta}{\Sigma}\right) d\phi^2 \quad (5)$$

$$2\rho = \frac{2Mr^3}{(r^2 + g^2)^{3/2}} - \omega \ln \frac{r}{|\omega|} \quad (6)$$

$$\Sigma = r^2 + a^2 \cos^2\theta, \quad (7)$$

$$\Delta = r^2 + a^2 - \frac{2Mr^4}{(r^2 + g^2)^{3/2}} + \omega r \ln \frac{r}{|\omega|} \quad (8)$$

The logrmetric term with ω parameter represents the role of PFDM to Bardeen metric. Solving $\Delta = 0$ gives us the Blackhole Event Horizon. On further examining we find that the black hole contains two event horizons, one very close to $r = 0$. The number of horizons present in a blackhole does not depend on the PFDM but the structure of spacetime and geodesic nature are affected by this PFDM term.

Photon orbits

We can derive the equations for photon orbit using Hamilton-Jacobi variable separation method. The Hamilton-Jacobi equation has a general form of.

$$\frac{\partial S}{\partial \lambda} = -\frac{1}{2}g^{\mu\nu} \frac{\partial S}{\partial x^\mu} \frac{\partial S}{\partial x^\nu} \quad (9)$$

where λ is the affine parameter and S corresponds to the Jacobi action

$$S = \frac{1}{2}m^2\lambda - Et + L\phi + S_r(r) + S_\theta(\theta) \quad (10)$$

where m is the rest mass, E and L are energy and Angular momentum which are the constants of motion.

Photon orbits

Solving this will yield us a separable equation,

$$\begin{aligned} & \frac{4\rho r a E L}{2\rho r(-a^2 - r^2 + a^2 \sin^2\theta) + (a^2 + r^2)\Sigma} \\ & + \frac{L^2(-2\rho r + \Sigma)}{\sin^2\theta(2\rho r(-a^2 - r^2 + a^2 \sin^2\theta) + (a^2 + r^2)\Sigma)} \\ & - \frac{E^2(a^2 2\rho r \sin^2\theta + (a^2 + r^2)\Sigma)}{2\rho r(-a^2 - r^2 + a^2 \sin^2\theta) + (a^2 + r^2)\Sigma} + \frac{\Delta_r}{\Sigma} S'_r{}^2 + \frac{S'_\theta{}^2}{\Sigma} = 0 \end{aligned} \quad (11)$$

This gives us two separate equations,

$$S'_r = \frac{\sqrt{R}}{\Delta_r}, S'_\theta = \sqrt{\Theta} \quad (12)$$

Where,

$$R = (aL - (a^2 + r^2)E)^2 - (K + (aE - L)^2)\Delta_r \quad (13)$$

$$\Theta = K - \left(\frac{L^2}{\sin^2\theta} - a^2 E^2\right) \cos^2\theta \quad (14)$$

Photon orbits

Now, we can write the geodesic motion as,

$$\Sigma \dot{t} = \frac{((r^2 + a^2)E - aL)(r^2 + a^2)}{\Delta_r} - a(aE \sin^2 \theta - L) \quad (15)$$

$$\Sigma \dot{r} = \sqrt{R} \quad (16)$$

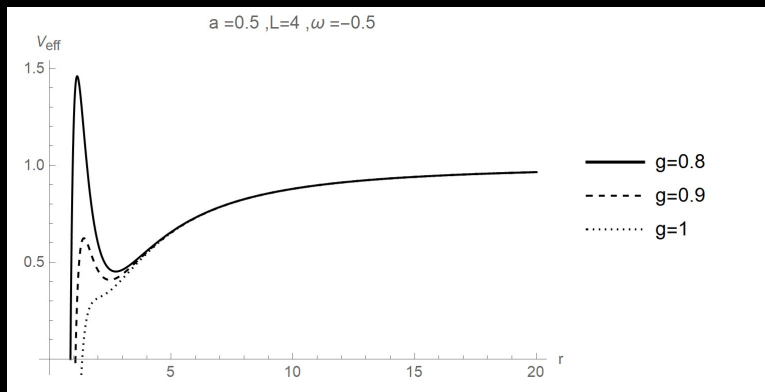
$$\Sigma \dot{\theta} = \sqrt{\theta} \quad (17)$$

$$\Sigma \dot{\phi} = \frac{a((r^2 + a^2)E - aL)}{\Delta_r} - \frac{aE \sin^2 \theta - L}{\sin^2 \theta} \quad (18)$$

Photon orbits

Effective potential can be obtained from the radial equation,

$$\dot{r}^2 + V_{\text{eff}} = E^2 \quad (19)$$



Photon orbits

using,

$$\xi = L/E, \eta = K/E^2 \quad (20)$$

rewriting (25) and (26)

$$R_p = (a\xi - (a^2 + r^2))^2 - (\eta + (a - \xi))\Delta_r \quad (21)$$

$$\Theta_p = \eta - \left(\frac{\xi^2}{\text{Sin}^2\theta} - a^2\right)\text{Cos}^2\theta \quad (22)$$

a photon would have zero radial velocity and zero radial acceleration to have a spherical orbit,

$$R_p = 0, \frac{dR_p}{dr} = 0 \quad (23)$$

Photon orbits

Using (32) and (35), we derive..

$$\xi = \frac{-4r\Delta_r + a^2\Delta'_r + r^2\Delta''_r}{a\Delta'_r} \quad (24)$$

$$\eta = \frac{r^2(16a^2\Delta_r - 16\Delta_r^2 + 8r\Delta_r\Delta'_r - r^2\Delta_r'^2)}{a^2\Delta_r'^2} \quad (25)$$

ξ and η are the impact parameters.

The celestial co-ordinates where derived using geodesic equations, and there are written in the function of impact parameters,

$$\alpha = -\frac{\xi}{\text{Sin}\theta_0} \quad (26)$$

$$\beta = \pm\sqrt{\eta + a^2\text{Cos}^2\theta_0 - \xi^2\text{Cot}^2\theta_0} \quad (27)$$

Shadows

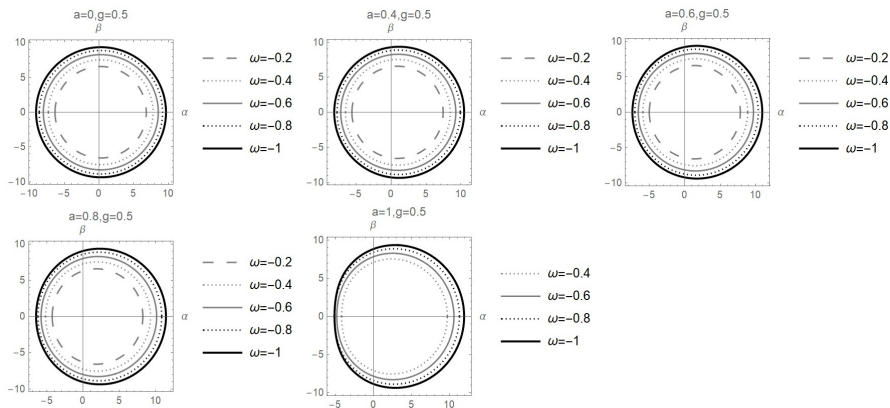


Figure: Shadow with constant g and change in a and δ

Shadows

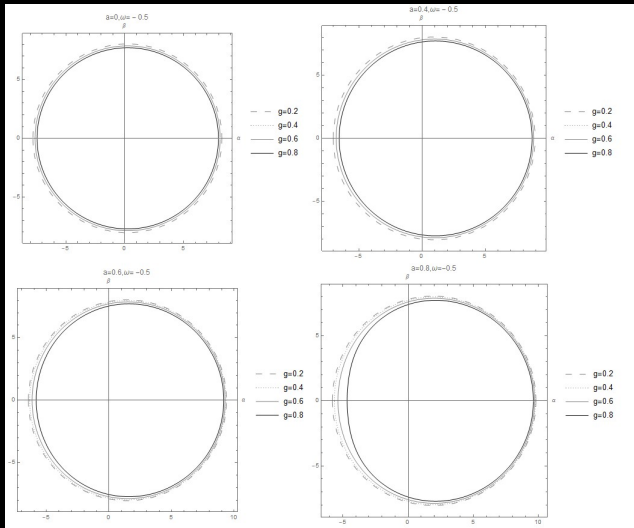


Figure: Shadow with constant δ and change in a and g

Points to Remember

- For a constant g , the size of shadow decreases with increase in dark matter parameter ω
- For a constant g , the distortion of the shadow increases with increase in spin parameter a
- For a constant ω , Although there is no significant change in shadow size, the distortion caused by spin parameter a is prominent with increase in g .

Bardeen Blackhole in PFDM immersed in Plasma

- Since almost all blackholes are in a sea high energy charged material medium, It is only logical to immerse our non-singular blackhole surrounded by PFDM in a plasma medium.
- the plasma medium can be both magnetised and non-magnetised. For simplification we are consider the plasma to be non-magnetized, pressureless the and non-interacting with the PFDM.
- The Hamiltonian for light rays in presence of plasma is expressed as,

$$H(x^\mu, p_\mu) = \frac{1}{2}[g^{\mu\nu} p_\mu p_\nu + \psi_p(r)^2] \quad (28)$$

where $\psi_p(r)$ is the plasma frequency and it has considered to be dependent on radial parameter alone.

- The refractive index (n) of the plasma medium can be written with the plasma frequency (ψ_p) and the frequency of photons (ψ) as measured by a non-moving observer. The expression for refractive index ($n(r, \psi)$) is given as,

$$n^2(r, \psi) = 1 - \left(\frac{\psi_p(r)}{\psi} \right)^2 \quad (29)$$

- The effective energy of the photon as measured by the observer is $\hbar\lambda\psi = -p_\mu u^\mu$, where u^μ is the 4-velocity. Since the observer is non-moving, we have $\hbar\lambda\psi = -p_0 u^0 = -p_0 \sqrt{-g^{00}}$. Now with (28) and (29), we get the expression for Hamiltonian as,

$$H(x^\mu, p_\mu) = \frac{1}{2} \left[g^{\mu\nu} p_\mu p_\nu - (n^2 - 1) (-p_0 \sqrt{-g^{00}})^2 \right] \quad (30)$$

- where,

$$n(r) = \sqrt{1 - \frac{k}{r^h}} \quad (31)$$

- where, k is a constant that gives the weightage of plasma around the black hole. h can take integer values greater than equal to zero.
- For $h = 0$ will result in $n(r) = \text{constant}$ that corresponds to homogenous plasma medium. Another case is a Inhomogeneous plasma distribution with basic dependence on r with $h = 1$. Both cases has been considered in this study.

Blackhole shadow in plasma medium

- In this section we are going to calculate the shadows of the blackhole.
- Shadows are result of strong gravitational lensing of photons by a blackhole. photons circle around the blackhole in an unstable circular orbit. when these rays reach the observer they form a distinctive circular or distorted boundary.
- In order to calculate the shadow we need to calculate the photon geodesics for an orbitary plane. which could be done using Hamilton - Jacobi variable seperation method the hamilton jacobi equation reads as,

$$-\mathcal{H} = \frac{\partial \mathcal{S}}{\partial \lambda} = -\frac{1}{2} \left[g^{\mu\nu} \frac{\partial \mathcal{S}}{\partial x^\mu} \frac{\partial \mathcal{S}}{\partial x^\nu} + (n^2 - 1)g^{00} \left(\frac{\partial \mathcal{S}}{\partial x^0} \right) \right] \quad (32)$$

where λ is the affine parameter and \mathcal{S} corresponds to the Jacobi action

Blackhole shadow in plasma medium

- the jacobian action is given by,

$$S = \frac{1}{2}m^2\lambda - Et + L\phi + S_r(r) + S_\theta(\theta) \quad (33)$$

where m is the rest mass, E and L are energy and Angular momentum which are the constants of motion.

- by solving this one simply arrives at

$$\Delta \left(\frac{\partial S_r}{\partial r} \right)^2 + \left(\frac{\partial S_\theta}{\partial \delta} \right)^2 - \frac{(n^2 - 1)}{\Delta} E^2 (r^2 + a^2) - \frac{1}{\Delta} [(r^2 + a^2)E - aL]^2 - (n^2 - 1)a^2 E^2 + (aE - L)^2 = 0 \quad (34)$$

Blackhole shadow in plasma medium

- the solution for S_r and S_δ yields,

$$\left(\frac{\partial S_\delta}{\partial \delta}\right)^2 = -\Delta \left(\frac{\partial S_r}{\partial r}\right)^2 - \frac{(n^2 - 1)}{\Delta} E^2 (r^2 + a^2) \quad (35)$$
$$+ \frac{1}{\Delta} [(r^2 + a^2)E - aL]^2 - (n^2 - 1)a^2 E^2 - (aE - L)^2 = \mathcal{K}$$

- The equations for r and δ can be obtained using $\frac{\partial \mathcal{L}}{\partial \dot{x}^\mu} = \frac{\partial S}{\partial x^\mu}$, where \mathcal{L} is the Lagrangian

$$r^2 \dot{r} = \sqrt{\mathcal{R}(r)} \quad (36)$$

$$r^2 \dot{\delta} = \sqrt{\Theta(\delta)} \quad (37)$$

where \mathcal{K} is the the separation constant

Blackhole shadow in plasma medium

- The trajectory of a photon is calculated with the two chandrasekar constant ,

$$\xi = \frac{L}{E}, \eta = \frac{\mathcal{K}}{E^2} \quad (38)$$

- Rewriting the impact parameters as a function r ,

$$\xi(r) = \frac{a^2\Delta' + r^2\Delta' - 4r\Delta(r)}{a\Delta'}; \quad (39)$$

$$\eta = \frac{r^2(16a^2\Delta - r^2\Delta'^2 - 16\Delta^2 + 8r\Delta\Delta')}{a^2\Delta'^2} \quad (40)$$

Blackhole shadow in plasma medium

- A blackhole shadow is essentially a dark disk-like region in a bright background and is essentially a planar image which can be defined by two coordinates.
- The coordinates that are applied to an infinite observer is called the celestial coordinates (α, β) .
- The celestial coordinates are expressed as follow,

$$\alpha = \lim_{r_0 \rightarrow \infty} \left(-r_0^2 \sin\theta \frac{d\phi}{dr} \right) \quad (41)$$

$$\beta = \lim_{r_0 \rightarrow \infty} \left(-r_0^2 \frac{d\theta}{dr} \right) \quad (42)$$

- Black hole shadow can be obtained by plotting α against β on X and Y -axes respectively,

Blackhole shadow in plasma medium

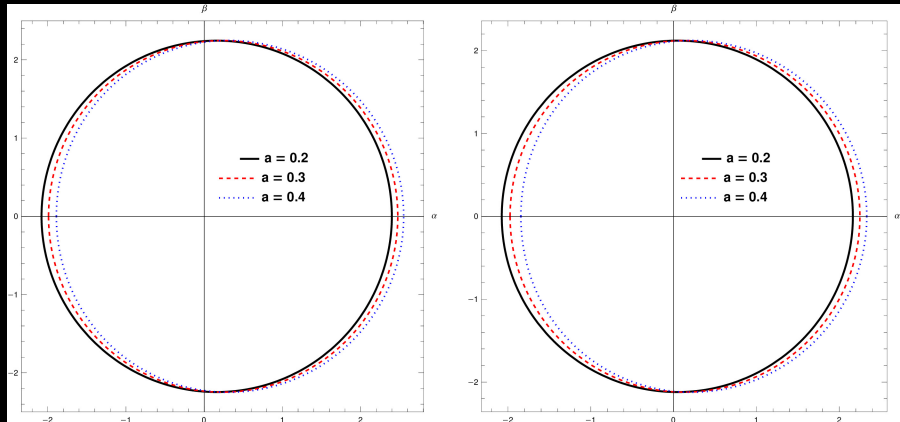


Figure: Shadow of black hole for varying spin parameter with $g = 0.2, k = 0.2$ and lower range $\omega = 0.2$ (left) and upper range $\omega = 1$ (right), Coloured plots show different values of spin parameter values - black ($a = 0.2$), red dashed ($a = 0.3$), blue dotted ($a = 0.4$)

Blackhole shadow in plasma medium

In the Fig.2. we have show the shadow of black hole with varying spin and constant magnetic monopole and plasma parameter. the shadow is obtained in both lower and upper regions of PFDM parameter. From the plot ,the distortion caused by the spin parameter seems to be more prominent in $\omega > \omega_c$ region than $\omega < \omega_c$. The distortion effect seen here is a result of rotational drag on the photon orbits. Also the size of the shadows are smaller in upper region than lower.

Blackhole shadow in plasma medium

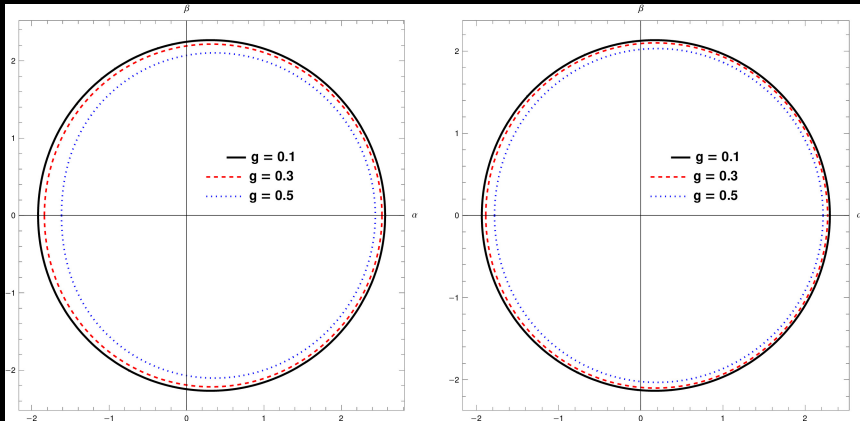


Figure: Shadow of black hole for varying magnetic monopole parameter with $a = 0.4, k = 0.2$ and lower range $\omega = 0.2$ (left) and upper range $\omega = 1$ (right), Coloured plots show different values of spin parameter values - black ($g = 0.1$), red dashed ($g = 0.3$), blue dotted ($g = 0.5$)

Blackhole shadow in plasma medium

In Fig.3 we have shown the effect of magnetic monopole g in the shadows, as discussed earlier we have two cases one with $\omega < \omega_c$ region (left) and the other with $\omega > \omega_c$ (right) region. In the $\omega < \omega_c$ region we can see that as g value increases the shadow gets more and more distorted. This distortion effect can also be seen in $\omega > \omega_c$ region but it is not as pronounced as it is in $\omega < \omega_c$ region.

Blackhole shadow in plasma medium

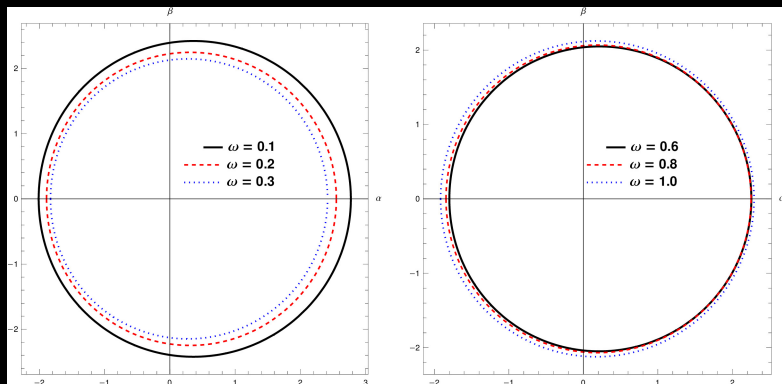


Figure: Shadow of black hole for varying PFDM parameter with $a = 0.4$, $g = 0.2$, $k = 0.2$. PFDM parameter at the lower range are depicted in the left and upper region are depicted in right

Blackhole shadow in plasma medium

In Fig.4, the shadow is plotted for a blackhole with constant spin, magnetic moment and plasma parameter with varying PFDM parameter. similar to last plot we have two cases namely lower $\omega < \omega_c$ region and upper $\omega > \omega_c$ region. As the PFDM values increase in $\omega < \omega_c$ region we can see a reduction in size of the shadow . On the Contrary , in $\omega > \omega_c$ region as PDFM value increases the size of the shadow also increases.

Blackhole shadow in plasma medium

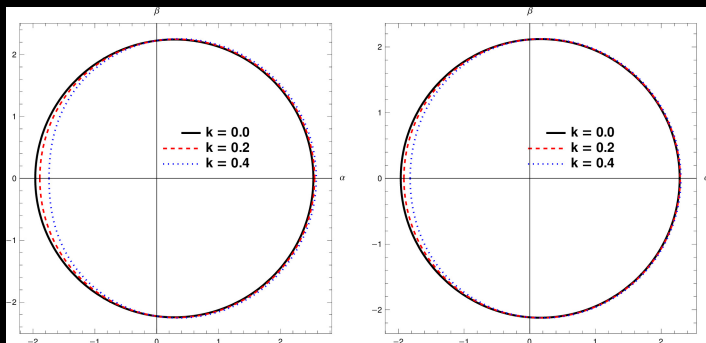


Figure: Shadow of black hole in homogenous plasma medium with $a=0.4$, $g = 0.2$ and lower range $\omega = 0.2$ (left) and upper range $\omega = 1$ (right), Coloured plots show different values of plasma parameter values - black ($k = 0.0$), red dashed ($k = 0.2$), blue dotted ($k = 0.4$)

Blackhole shadow in plasma medium

In Fig 5, the shadow is plotted for a homogeneous plasma medium with varying plasma parameter and constant spin and magnetic moment. We have plotted in two cases with $\omega = 0.2$ in $\omega < \omega_c$ and with $\omega = 1$ in $\omega > \omega_c$ region. From the plot it is seen that as plasma parameter increases there is a visible deformation in the shadow but the deformations are more prominent in the $\omega < \omega_c$ than in the $\omega > \omega_c$ region.

Blackhole shadow in plasma medium

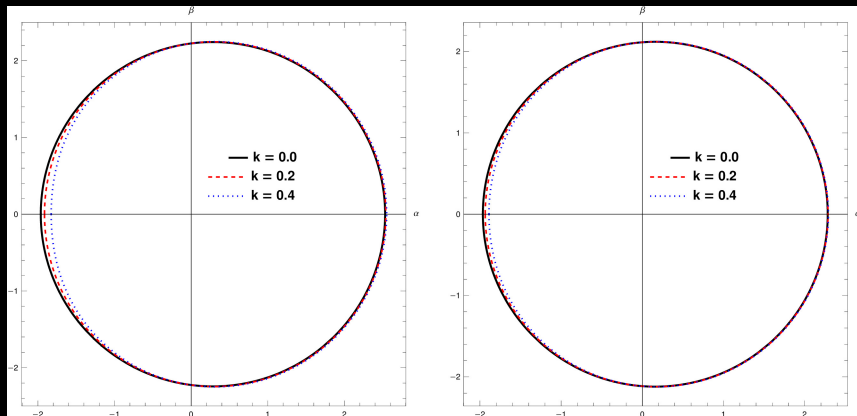


Figure: Shadow of black hole in inhomogenous plasma medium with $a=0.4$, $g = 0.2$ and lower range $\omega = 0.2$ (left) and upper range $\omega = 1$ (right), Coloured plots show different values of plasma parameter values - black ($k = 0.0$), red dashed ($k = 0.2$), blue dotted ($k = 0.4$)

Blackhole shadow in plasma medium

In Fig 6, the shadow plot is similar to that of in Fig 6 but with an inhomogenous plasma medium. there is evidence of deformation in both regions. it is to mention that the deformation in $\omega > \omega_c$ is nearly insignificant. Comparing Fig 5 with Fig 6 , evidently the deformation in homogenous plasma medium is more distinguished than in inhomogenous plasma medium.

Effective Potential

The unstable and stable orbits are the result of Maxima and minima of the effective potential, Maxima is given by $\frac{\partial^2 V_{\text{eff}}}{\partial r^2} < 0$ and minima as $\frac{\partial^2 V_{\text{eff}}}{\partial r^2} > 0$, the expression for effective potential is given as.

$$\dot{r}^2 + V_{\text{eff}} = E \quad (43)$$

where \dot{r} is defined as

$$\dot{r}^2 = \frac{1}{r^4} [(E^2(r^2 + a^2) - aL)^2 - \Delta(aE - L)^2 + (n^2 - 1)(E^2(r^2 + a^2))^2 - \Delta E^2] \quad (44)$$

Except plasma parameter all other are kept constant, the plot for effective potential vs r has been plotted with two cases, one lower range $\omega < \omega_c$ and other upper range $\omega > \omega_c$

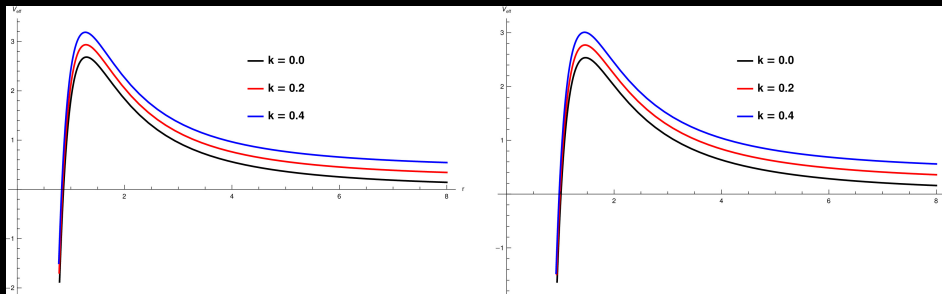


Figure: Variation of effective potential with plasma parameter in an homogenous plasma medium with $a = 0.4, L = 3$ and $g = 0.5$, the left panel is of lower range with $\omega = 0.2$ and right panel is of upper range with $\omega = 1$

Fig 7 shows the effective potential a photon faces while orbiting a blackhole. the effective potential here is presented with a variation in plasma parameter k . the distribution here is considered to be homogenous so that $n = \sqrt{1 - k}$. The left pannel is $\omega = 0.2$ and right is with $\omega = 1$. the plots are done with futher consideration of $M = 1, a = 0.4, E = 1, L = 3$ and $g = 0.5$. It is to be noted that in both cases the potential increases uniformly as we increase the plasma parameter. The Maxima in the potential denotes the presence of unstable orbits. the position of maxima moves slightly towards the left as the plasma parameter increases.

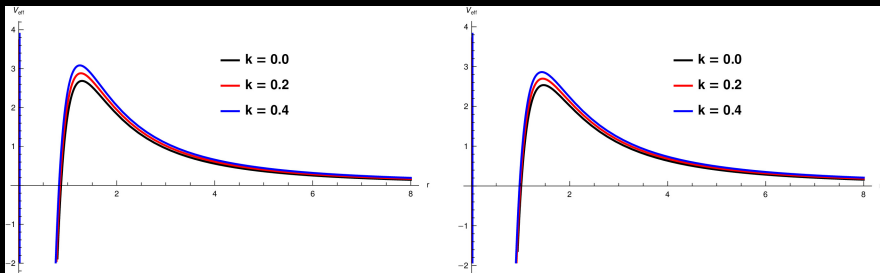


Figure: Variation of effective potential with plasma parameter in inhomogeneous plasma medium with $a = 0.4, L = 3$ and $g = 0.5$, the left panel is of lower range with $\omega = 0.2$ and right panel is of upper range with $\omega = 1$

Fig 8 shows the effective potential a photon faces while orbiting a blackhole. the effective potential here is presented with a variation in plasma parameter k . the distribution here is considered to be inhomogenous so that $n(r) = \sqrt{1 - \frac{k}{r}}$. The left pannel is $\omega = 0.2$ and right is with $\omega = 1$. Similar to homogenous medium the potential increases uniformly in both regions as the plasma parameter increases. The Maxima in the potential denotes the presence of unstable orbits. the position of maxima moves slightly towards the left as the plasma parameter increases and also the maxima shifts towards the left. The uniform increase in effective potential in both plasma distribution suggests that the presence plasma increases the total mass of the system. which means that the total energy of the system also increases with the presence of plasma.

Summary

- The system under consideration here is an rotating non-singular magnetic monopole in Perfect Fluid Dark Matter. Further, we immerse this system in plasma with radial plasma distribution. we have assumed that there is no interaction between the plasma and PFDM.
- Firstly we see a peculiar characteristic related to the PFDM presence. we find that the outer event horizon decreases with increase in PFDM parameter to a particular critical value. beyond this critical value the outer event horizon starts to increase again, Since mass plays a major role in event horizon we conclude that this peculiarity is due to the added mass of PFDM which after certain point dominates the mass the blackhole.

- The plasma and PFDM are assumed to non-interacting with each other in nature hence they dont directly affect each other. we have two cases of plasma medium under consideration, homogenous plasma distribution with $n = \sqrt{1 - k}$ and inhomogenous plasma distribution with $n(r) = \sqrt{1 - \sqrt{kr}}$. we have studied the null geodesics and using the geodesic equation we have caluclated the celestial coordinates (α, β) the blackhole shadow is formed on this clestial plane and the shadow radius can be easily obtained as $R_S^2 = \alpha^2 + \beta^2$
- The blackhole shadow has been analysed with the blackhole parameter Spin a ,Magnetic moment g ,PFDM parameter ω and plasma parameter k .as expected the shadow gets deformed with with increased rotational drag,and as well as with increased magnetic moment.whereelse the size of the shadow decreases with increase in PFDM parameter till $\omega < \omega_c$ and beyond $\omega > \omega_c$ the shadow size starts to increase.

- Photons encircling the blackhole in an unstable orbit travel through vacuum, when a photon travel in a medium it gets deviated and this deviation depends on the refractive index of the medium.
- similarly when photon travel through plasma it get deviated and it depends on plasma frequency. the variation caused by this plasma medium affects the shadow radius of the black hole.
- Effective potential is the potential encountered by the photon orbiting the blackhole, studying this effective potential we have found a strong dependence on the plasma parameter as the maxima shifts towards the left as the plasma parameter increases. also the peak maxima increases with the increase in plasma parameter. as discussed earlier the reason for increasing maxima is the account of increased plasma mass and by then increasing the total energy of the system.

References

- James M Bardeen. Non-singular general-relativistic gravitational collapse. In Proc. Int. Conf. GR5, Tbilisi, volume 174, 1968
- Eloy Ayon-Beato and Alberto Garcia. The Bardeen model as a nonlinear magnetic monopole. Physics Letters B, 493(1-2):149–152, 2000
- He-Xu Zhang, Yuan Chen, Peng-Zhang He, Qi-Qi Fan, and Jian-Bo Deng. Bardeen black hole surrounded by perfect fluid dark matter. arXiv preprint arXiv:2007.09408, 2020.
- VV Kiselev. Quintessential solution of dark matter rotation curves and its simulation by extra dimensions. arXiv:gr-qc/0303031, 2003.
- Ming-Hsun Li and Kwei-Chou Yang. Galactic dark matter in the phantom field. Physical Review D, 86(12):123015, 2012.
- Xian Hou, Zhaoyi Xu, and Jiancheng Wang. Rotating black hole shadow in perfect fluid dark matter. Journal of Cosmology and Astroparticle Physics, 2018(12):040, 2018.

Thank you